Metamagnetic Copper(II) Diphosphonates with Layered Structures

Li-Min Zheng,*,† Song Gao,‡ Hui-Hua Song,† Silvio Decurtins,§ Allan J. Jacobson,|| and Xin-Quan Xin†

State Key Laboratory of Coordination Chemistry, Coordination Chemistry Institute, Nanjing University, Nanjing 210093, P. R. China, State Key Laboratory of Rare Earth Materials and Applications, College of Chemistry and Molecular Engineering, Peking University, Beijing 100871, P. R. China, Department of Chemistry and Biochemistry, Bern University, Bern, Switzerland, and Department of Chemistry, University of Houston, Houston, Texas 77204

Received February 11, 2002. Revised Manuscript Received April 18, 2002

Compounds $[NH_3(CH_2)_4NH_3]Cu_3(hedp)_2{\cdot}2H_2O$ (**1**) and $[NH_3(CH_2)_3NH_3]Cu_3(hedp)_2{\cdot}3.5H_2O$ (**2**), where hedp represents 1-hydroxyethylidenediphosphonate, exhibit two-dimensional structures closely related to each other. The anionic layers with composition $\{Cu_3(hedp)_2\}_n^{2n-}$ contain four- and eight-membered rings assembled from vertex-sharing $\{CuO_4\}$ units and $\{CPO_3\}$ tetrahedra. The protonated diamines and lattice water fill the interlayer spaces. Crystal data for **2**: space group $P\bar{1}$, $a = 8.0315(4)$, $b = 11.3713(6)$, $c = 13.3117(7)$ Å, $\alpha = 97.122(1)$, $\beta = 103.187(1)$, $\gamma = 108.668(1)°$, $V = 1095.5(1)$ Å^3, $Z = 2$. Magnetic properties of the two compounds have been investigated. Both show typical metamagnetic behaviors at low temperature. The critical field at which the antiferromagnetic ground-state switches to a ferrimagnetic state is ∼48 Oe for **1** and 185 Oe for **2** at about 2 K.

Introduction

Metal phosphonate materials are of increasing interest due to their potential applications in exchange, sorption, catalysis, and so forth.[1] Major efforts have been devoted to the exploration of novel phosphonate compounds with open framework or porous structures.[2] With the aim of finding new insulators that might order ferromagnetically, investigations have been carried out on some phosphonate compounds with layered or pillared−layered structures and with other structure types. Although no true ferromagnet has yet been discovered in a phosphonate system, interesting weak ferromagnetism (canted antiferromagnetism) was observed in $Fe(RPO_3){\cdot}H_2O$ ($R = C_2H_5$, C_6H_5),[3,4] $Cr(CH_3PO_3){\cdot}H_2O$,[5] $Mn(C_nH_{2n+1}PO_3){\cdot}H_2O$,[6] $Co_3(O_3PC_2H_4CO_2)_2$,[7] and $\{K_2[CoO_3PCH_2N(CH_2CO_2)_2]\}_6{\cdot}xH_2O$.[8] Very recently, we described a three-dimensional copper phosphonate, $Cu_4(hedp)_2(pz)(H_2O)_2$ [hedp = 1-hydroxyethylidenediphosphonate, $CH_3C(OH)(PO_3)_2$, pz = pyrazine], which shows metamagnetism at low temperature.[9] In this paper, we report the magnetic properties of two layered copper diphosphonates: $[NH_3(CH_2)_4NH_3]Cu_3(hedp)_2{\cdot}2H_2O$ (**1**) and $[NH_3(CH_2)_3NH_3]Cu_3(hedp)_2{\cdot}3.5H_2O$ (**2**), where the $\{Cu_3(hedp)_2\}_n^{2n-}$ layers are separated by $[NH_3(CH_2)_nNH_3]^{2+}$ cations and lattice water. Both show interesting metamagnetic behaviors.

Experimental Section

Materials and Methods. All of the starting materials were reagent grade and used as purchased. The 50% aqueous solution of 1-hydroxyethylidenediphosphonic acid ($hedpH_4$) was purchased from Nanjing Shuguang Chemical Factory of China. The elemental analyses were performed on a PE 240C elemental analyzer. The infrared spectra were recorded on a Nicolet 170SX FT-IR spectrometer with pressed KBr pellets. The magnetic susceptibility measurements for **1**−**2** were carried out on polycrystalline samples (44.9 mg for **1**, 36.7 mg for **2**) using a MagLab System 2000 magnetometer in a magnetic field up to 7 T. Diamagnetic corrections were estimated from Pascal's constants.[10]

* To whom correspondence should be addressed. E-mail: lmzheng@netra.nju.edu.cn; Fax: +86−25−3314502.

† State Key Laboratory of Coordination Chemistry, Coordination Chemistry Institute, Nanjing University.

‡ State Key Laboratory of Rare Earth Materials and Applications, College of Chemistry and Molecular Engineering, Peking University.

§ Department of Chemistry and Biochemistry, Bern University.

|| Department of Chemistry, University of Houston.

(1) Cao, G.; Hong, H.; Mallouk, T. E. *Acc. Chem. Res.* **1992**, *25*, 420. Alberti, G. *Comprehensive Supramolecular Chemistry*; Lehn, J. M., Ed.; Pergamon: Elsevier Science, Ltd.: Oxford, U. K., 1996; Vol. 7. Snover, J. L.; Byrd, H.; Suponeva, E. P.; Vicenzi, E.; Thompson, M. E. *Chem. Mater.* **1996**, *8*, 1490. Johnson, J. W.; Jacobson, A. J.; Butler, W. M.; Rosenthal, S. E.; Brody, J. F.; Lewandowski, J. T. *J. Am. Chem. Soc.* **1989**, *111*, 381.

(2) Clearfield, A. *Progress in Inorganic Chemistry*; Karlin, K. D., Ed.; John Wiley & Sons: New York, 1998; Vol. 47, 371−510. Le Bideau, J.; Payen, C.; Palvadeau, P.; Bujoli, B. *Inorg. Chem.* **1994**, *33*, 4885. Lohse, D. L.; Sevov, S. C. *Angew. Chem., Int. Ed. Engl.* **1997**, *36*, 1619. Bonavia, G.; Haushalter, R. C.; O'Connor, C. J.; Sangregorio, C.; Zubieta, J. *Chem. Commun.* **1998**, 2187.

(3) Bujoli, B.; Pena, O.; Palvadeau, P.; Le Bideau, J.; Payen, C.; Rouxel, J. *Chem. Mater.* **1993**, *5*, 583.

(4) Bellitto, C.; Federici, F.; Altomare, A.; Rizzi, R.; Ibrahim, S. A. *Inorg. Chem.* **2000**, *39*, 1803.

(5) Bellitto, C.; Federici, F.; Ibrahim, S. A. *Chem. Commun.* **1996**, 759.

(6) Carling, S. G.; Visser, D.; Kremer, R. K. *J. Solid State Chem.* **1993**, *106*, 111.

(7) Rabu, P.; Janvier, P.; Bujoli, B. *J. Mater. Chem.* **1999**, *9*, 1323.

(8) Gutschke, S. O. H.; Price, D. J.; Powell, A. K.; Wood, P. T. *Angew. Chem., Int. Ed. Engl.* **1999**, *38*, 1088.

(9) Yin, P.; Zheng, L.-M.; Gao, S.; Xin, X.-Q. *Chem. Commun.* **2001**, 2346.

(10) Kahn, O. *Molecular Magnetism*; VCH Publishers: New York, 1993.

10.1021/cm020204+ CCC: $22.00
Published on Web 06/13/2002

Table 1. Crystallographic Data

compound	**2**
formula	$C_7\ H_{27}\ Cu_3\ N_2\ O_{17.50}\ P_4$
M	733.81
crystal system	triclinic
space group	$P\bar{1}$
a/Å	8.0315(4)
b/Å	11.3713(6)
c/Å	13.3117(7)
α/deg	97.1220(10)
β/deg	103.1870(10)
γ/deg	108.6680(10)
V/Å^3	1095.53(10)
Z	2
D_c/g cm^{-3}	2.225
F(000)	740
μ(Mo−Kα)/cm^{-1}	32.65
goodness of fit on F^2	1.337
R_1, wR_2[a] [$I>2\sigma(I)$]	0.0473, 0.1036
(all data)	0.0540, 0.1055
extinction efficient	0.0030(2)
$(\Delta\rho)_{max}$, $(\Delta\rho)_{min}$/e Å^{-3}	0.720, −0.957

[a] $R_1 = \sum||F_o|-|F_c||/\sum|F_o|$. $wR_2 = [\sum w(F_o^2-F_c^2)^2/\sum w(F_o^2)^2]^{1/2}$.

Table 2. Atomic Coordinates and Equivalent Isotropic Displacement Parameters (Å^2) for 2[a]

atom	x	y	z	$U_{(eq)}$
Cu(1)	0.2416(1)	0.2348(1)	0.7394(1)	0.018(1)
Cu(2)	0.2895(1)	0.0687(1)	1.0641(1)	0.014(1)
Cu(3)	0.2129(1)	0.4405(1)	0.4317(1)	0.014(1)
P(1)	0.0372(2)	0.0297(2)	0.8508(1)	0.013(1)
P(2)	0.4237(2)	0.0651(2)	0.8672(1)	0.014(1)
P(3)	0.0651(2)	0.4179(2)	0.6242(1)	0.015(1)
P(4)	0.4544(2)	0.4546(2)	0.6445(1)	0.014(1)
O(1)	0.0370(6)	0.1088(4)	0.7674(4)	0.020(1)
O(3)	−0.1554(6)	−0.0689(4)	0.8312(3)	0.016(1)
O(2)	0.1133(6)	0.1089(4)	0.9629(3)	0.016(1)
O(4)	0.4167(6)	0.1564(5)	0.7942(4)	0.022(1)
O(5)	0.4711(6)	0.1294(4)	0.9842(3)	0.016(1)
O(6)	0.5542(7)	−0.0013(5)	0.8475(4)	0.021(1)
O(7)	0.1887(7)	−0.1303(4)	0.9169(4)	0.018(1)
O(8)	0.656(7)	0.3121(5)	0.6846(4)	0.023(1)
O(9)	0.0209(6)	0.3710(4)	0.5042(3)	0.018(1)
O(10)	−0.0666(6)	0.4794(5)	0.6514(4)	0.019(1)
O(11)	0.4489(6)	0.3645(4)	0.7207(4)	0.018(1)
O(12)	0.3777(6)	0.3848(4)	0.5290(3)	0.017(1)
O(13)	0.6473(6)	0.5536(4)	0.6693(3)	0.018(1)
O(14)	0.3092(7)	0.6236(5)	0.5941(4)	0.023(1)
C(1)	0.1912(9)	−0.0563(6)	0.8355(5)	0.014(1)
C(2)	0.1322(11)	−0.1406(7)	0.7260(6)	0.027(2)
C(3)	0.2982(9)	0.5372(6)	0.6663(5)	0.017(1)
C(4)	0.3514(11)	0.6070(7)	0.7809(6)	0.027(2)
N(1)	−0.2224(18)	0.2941(16)	0.7781(11)	0.025(3)
C(81)	−0.1170(20)	0.3265(15)	0.8893(13)	0.034(4)
C(82)	−0.1450(20)	0.4340(14)	0.9510(12)	0.027(3)
C(83)	−0.0580(20)	0.5625(14)	0.9207(13)	0.033(4)
N(2)	−0.0374(18)	0.6682(12)	1.0031(11)	0.030(3)
N(3)	−0.6510(60)	0.1460(30)	0.3880(20)	0.015(6)
C(71)	−0.5800(30)	0.0489(17)	0.3931(13)	0.043(5)
C(72)	−0.4180(30)	0.0810(20)	0.4870(17)	0.060(6)
C(73)	−0.4570(30)	0.0950(30)	0.5868(16)	0.073(8)
N(4)	−0.3071(17)	0.1086(12)	0.6807(9)	0.025(3)
O(3W)	0.2010(18)	0.6417(12)	1.1824(12)	0.036(3)
O(4W)	0.8345(19)	0.6501(12)	0.8854(9)	0.047(3)
O(5W)	−0.6480(60)	0.1720(30)	0.3800(30)	0.035(8)
O(1W)	0.3707(9)	0.3754(7)	0.9610(6)	0.054(2)
O(2W)	0.1269(9)	0.1215(6)	0.5289(5)	0.040(1)

[a] $U_{(eq)}$ is defined as one-third of the trace of the orthogonalized U_{ij} tensor.

Table 3. Selected Bond Lengths [Å] and Angles [deg] for 2

Cu(1)−O(11)	1.928(5)	Cu(1)−O(8)	1.946(5)
Cu(1)−O(1)	1.948(5)	Cu(1)−O(4)	1.950(5)
Cu(2)−O(6A)	1.928(5)	Cu(2)−O(2)	1.930(4)
Cu(2)−O(3B)	1.946(4)	Cu(2)−O(5)	1.995(4)
Cu(3)−O(13C)	1.933(4)	Cu(3)−O(10D)	1.943(5)
Cu(3)−O(12)	1.945(4)	Cu(3)−O(9)	2.005(5)
P(1)−O(1)	1.513(5)	P(1)−O(2)	1.520(5)
P(1)−O(3)	1.533(5)	P(2)−O(4)	1.513(5)
P(2)−O(6)	1.523(5)	P(2)−O(5)	1.541(5)
P(3)−O(10)	1.524(5)	P(3)−O(8)	1.528(5)
P(3)−O(9)	1.540(5)	P(4)−O(12)	1.525(5)
P(4)−O(13)	1.527(5)	P(4)−O(11)	1.527(5)
O(11)−Cu(1)−O(8)	94.89(19)	O(11)−Cu(1)−O(1)	176.5(2)
O(8)−Cu(1)−O(1)	85.8(2)	O(11)−Cu(1)−O(4)	85.41(19)
O(8)−Cu(1)−O(4)	179.7(2)	O(1)−Cu(1)−O(4)	93.95(19)
O(6A)−Cu(2)−O(2)	170.9(2)	O(6A)−Cu(2)−O(3B)	89.35(19)
O(2)−Cu(2)−O(3B)	92.31(19)	O(6A)−Cu(2)−O(5)	92.35(19)
O(2)−Cu(2)−O(5)	89.06(19)	O(3B)−Cu(2)−O(5)	160.48(19)
O(13C)−Cu(3)−O(10D)	89.83(19)	O(13C)−Cu(3)−O(12)	92.14(19)
O(10D)−Cu(3)−O(12)	171.5(2)	O(13C)−Cu(3)−O(9)	159.26(19)
O(10D)−Cu(3)−O(9)	92.49(19)	O(12)−Cu(3)−O(9)	88.58(19)
P(1)−O(1)−Cu(1)	129.7(3)	P(1)−O(3)−Cu(2B)	121.0(3)
P(1)−O(2)−Cu(2)	118.7(3)	P(2)−O(4)−Cu(1)	134.7(3)
P(2)−O(5)−Cu(2)	118.9(3)	P(2)−O(6)−Cu(2A)	133.6(3)
P(3)−O(8)−Cu(1)	135.8(3)	P(3)−O(9)−Cu(3)	119.1(3)
P(3)−O(10)−Cu(3D)	130.8(3)	P(4)−O(11)−Cu(1)	129.6(3)
P(4)−O(12)−Cu(3)	119.0(3)	P(4)−O(13)−Cu(3C)	120.7(3)

Symmetry transformations used to generate equivalent atoms: A: $-x+1, -y, -z+2$; B: $-x, -y, -z+2$; C: $-x+1, -y+1, -z+1$; D: $-x, -y+1, -z+1$.

Syntheses of Compounds 1−2. Compound **1** was prepared according to the methods previously reported.[11] Compound **2** was also synthesized under hydrothermal conditions. A mixture of $Cu(NO_3)_2{\cdot}3H_2O$ (1 mmol, 0.2451 g), an aqueous solution of 50% $hedpH_4$ (1 cm^3), LiF (1 mmol, 0.0263 g), and H_2O (8 cm^3), adjusted by 1,3-propanediamine to pH ≈ 3, was heated in a Teflon-lined autoclave (25 cm^3) at 140 °C for 5d. After slow cooling, needlelike blue crystals of compound **2** were obtained as a monophasic material. Yield: 61% based on Cu. Found (calcd.) for $C_7H_{27}Cu_3N_2O_{17.5}P_4$: C, 11.88 (11.45); H, 3.84 (3.68); N, 3.68 (3.82)%. IR (KBr, cm^{-1}): 3551m, 3428m, 3176m, 1605w, 1520w, 1446w, 1400w, 1092s, 1053s, 1003m, 955m, 817w, 685w, 592m, 497w, 450w, 424w. Thermal analysis of **2** showed a one-step decomposition below 220 °C. The weight loss (8.2%, 50−130 °C) is in agreement with the removal of 3.5 H_2O (calcd. 8.6%).

X-ray Crystallographic Analysis. A crystal of **2** with dimensions 0.30 × 0.08 × 0.06 mm was selected for indexing and intensity data collection at 293(2) K on a Siemens SMART platform diffractometer equipped with a 1 K CCD area detector at 298 K with monochromated Mo−Kα (λ = 0.71073 Å) radiation. A hemisphere of data (1271 frames at 5 cm detector distance) was collected using a narrow-frame method with scan widths of 0.30° in ω and an exposure time of 30 s/frame. The first 50 frames were remeasured at the end of data collection to monitor instrument and crystal stability, and the maximum correction applied on the intensities was <1%. The data were integrated using the Siemens SAINT program,[12] with the intensities corrected for Lorentz factor, polarization, air absorption, and absorption due to variation in the path length through the detector faceplate. Empirical absorption was applied.

The structure was solved by direct methods and refined on F^2 by full-matrix least squares using SHELXTL.[13] All the nonhydrogen atoms were refined anisotropically. All the hydrogen atoms were assigned fixed isotropic thermal parameters 1.2 or 1.4 or 1.5 times the equivalent isotropic U of the atoms to which they are attached, and were refined isotropically. The H atoms attached to O3w, O4w, and O5w were not located. Selected crystallographic data and structure determination parameters are given in Table 1, atomic coordinates in Table 2, and selected bond lengths and angles in Table 3.

(11) Zheng, L.-M.; Song, H.-H.; Duan, C.-Y.; Xin, X.-Q. *Inorg. Chem.* **1999**, *38*, 5061.

(12) *SAINT*, Program for Data Extraction and Reduction, Siemens Analytical X-ray Instruments Inc., Madison, WI, 1994−1996.

(13) Sheldrick, G. M. *SHELXTL PC*, version 5; Siemens Analytical X-ray Instruments Inc.: Madison, WI, 1995.

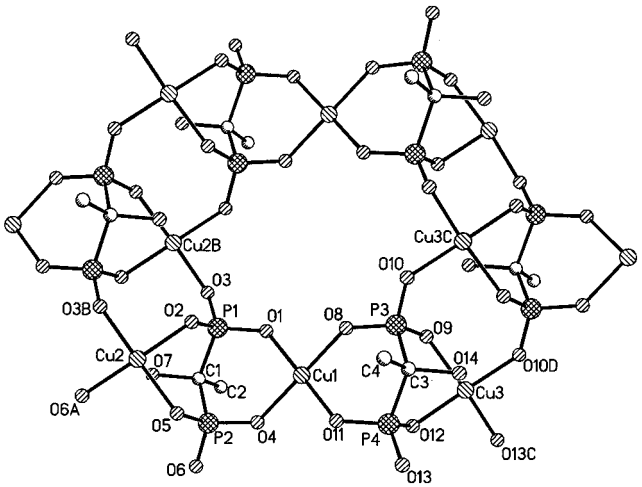

Figure 1. Fragment of the $\{Cu_3(hedp)_2\}_n^{2n-}$ layer in structure **2** with the atomic labeling scheme.

Results and Discussions

Crystal Structures. The structure of **1** has been described in a previous paper.[11] Compound **2** has a similar layered structure. It consists of a two-dimensional anionic layer of $\{Cu_3(hedp)_2\}_n^{2n-}$ and diprotonated 1,3-propanediamine pillars. Figure 1 shows the building unit of the layer with atomic labeling scheme. There are three crystallographically distinct Cu atoms. The Cu(1) atom is coordinated by four oxygen atoms provided by two different $hedp^{4-}$ groups in approximately square planar geometry. The mean deviation from the plane defined by the O(1), O(4), O(8), O(11), and Cu(1) atoms, is 0.0285 Å. Both Cu(2) and Cu(3) atoms have distorted tetrahedral environments, the four oxygen atoms of each are provided by three $hedp^{4-}$ groups. The Cu−O distances fall in the range of 1.928(5)−2.005(5) Å, similar to those in the other Cu-hedp compounds.[11,14]

Two kinds of $hedp^{4-}$ groups are observed in the structure, each of which acts as a bis(chelating) ligand to bridge two Cu atoms, thereby forming a $\{Cu_3(hedp)_2\}$ trimer (Figure 1). This trimer unit is asymmetrical in **2**, whereas a similar trimer is symmetrical in the layer compound **1**.[11] The remaining two phosphonate oxygen atoms coordinate to Cu(2) or Cu(3) from the neighboring trimers leading to the formation of a layer. The 1,3-propanediammonium cations and water molecules are located between the layers (Figure 2). The closest Cu...Cu distances in **2** are 4.240 Å within the layer and 6.333 Å between the layers. For compound **1**, the same distances are 4.247 and 6.211 Å, respectively.

Magnetic Properties. The temperature-dependent molar magnetic susceptibilities of compound **1** were investigated in a magnetic field of 20 kOe (Figure 3). The observed $\chi_M T$ value per Cu_3 unit at 300 K (1.16 cm^3 mol^{-1} K) is in accordance with the expected value (1.24 cm^3 mol^{-1} K) for three magnetically isolated Cu(II) ions ($S = 1/2$, $g = 2.1$). Upon cooling, compound **1** show the typical features of ferrimagnetic behavior. The $\chi_M T$ value decreases smoothly until it reaches a minimum of 0.68 cm^3 mol^{-1} K around 36 K, then increases abruptly to a maximum of 1.88 cm^3 mol^{-1} K at 8.6 K, suggesting the onset of magnetic ordering. The magnetic susceptibility above 50.0 K obeys the Curie−Weiss law for **1**, with a Weiss constant $\theta = -37$ K, confirming an antiferromagnetic coupling between the adjacent magnetic centers. The χ_M vs T curves of **1** measured at 20 kOe, 180 and 30 Oe show a sharp peak at ca. 4.7 K at a low field of 30 Oe (inset of Figure 3), suggesting the occurrence of long-range antiferromagnetic (AF) ordering. The transition temperature (T_N) is below 4.7 K.

The field dependent magnetization of compound **1** measured at 1.8 K, shown as Figure 4, reveals a metamagnetic behavior: Below ~50 Oe, the magnetization increases slightly with increasing field; subsequently, it increases abruptly to a ferrimagnetic state and reaches a saturation magnetization plateau above 5 kOe. The saturation magnetization at 50 kOe is 1.18 Nβ per Cu_3 unit, close to the value of 1.1 Nβ anticipated

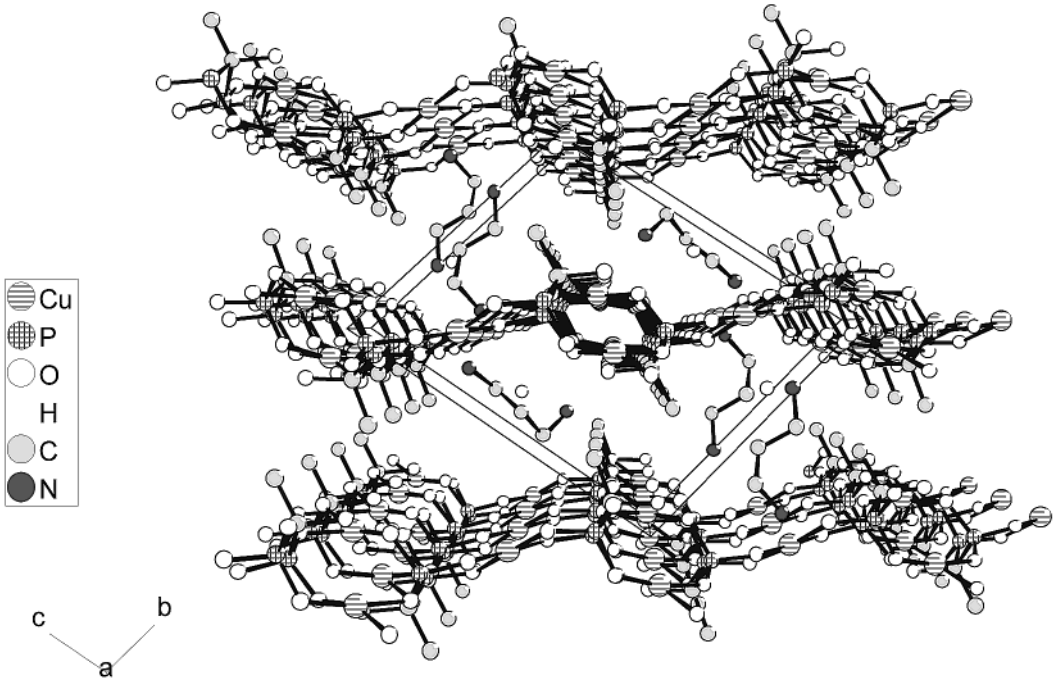

Figure 2. Packing diagram of structure **2** along [100] direction.

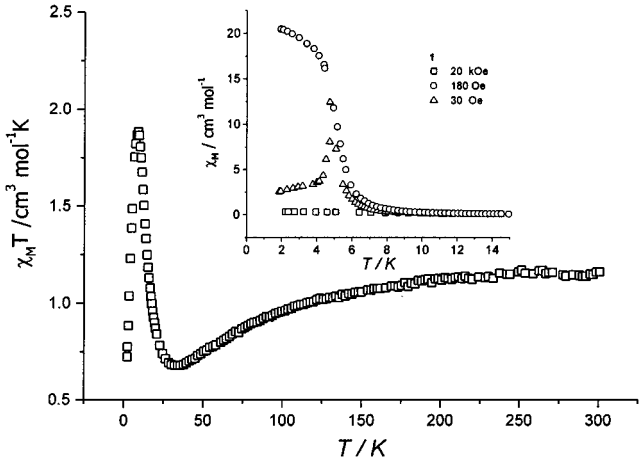

Figure 3. Temperature dependence of magnetic susceptibility of **1**: $\chi_M T$ (□) vs T plot at 20 kOe; inset, χ_M vs T plots at 20 kOe (□), 180 Oe (○), and 30 Oe (△).

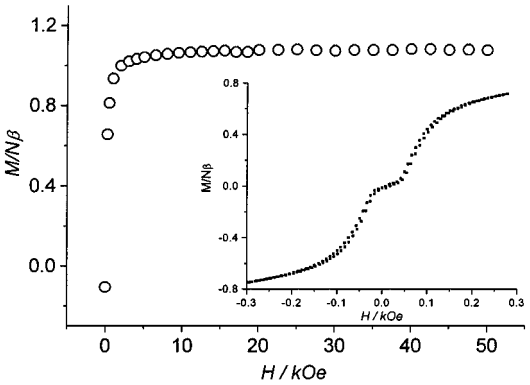

Figure 4. Field dependent magnetization and hysteresis loop (inset) for **1** at 1.8 K.

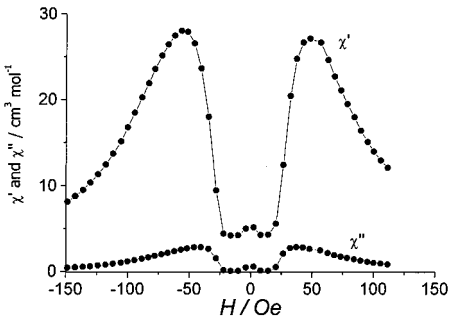

Figure 5. Field dependence of *ac* magnetization at 1.8 K for **1**.

for a net spin value of $S = {}^1/_2$ with $g = 2.1$. The hysteresis loop at 1.8 K is typical for a soft ferrimagnet. The field dependence of *ac* susceptibility measurement shows a critical field of ~48 Oe (Figure 5).

The ferrimagnetic behavior is also observed for compound **2** (Figure 6). A sharp peak appears in the χ_M vs T curve at ~6 K at low field (100 Oe), suggesting an AF ground state (inset of Figure 6). This AF ground state is confirmed by the temperature-dependent zero-field *ac* magnetic susceptibility $\chi_M'(T)$, which shows a magnetic phase transition at ca. 6.0 K at $H_{ac} = 5$ Oe and the absence of frequency dependence. The magnetization measurements of **2** at 1.94 K correspond to a

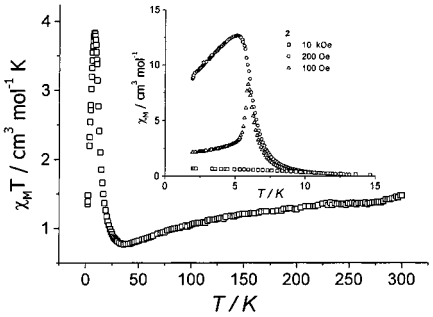

Figure 6. Temperature dependence of magnetic susceptibility of **2**: $\chi_M T$ (□) vs T plot at 10 kOe; inset, χ_M vs T plots at 10 kOe (□), 200 Oe (○), and 100 Oe (△).

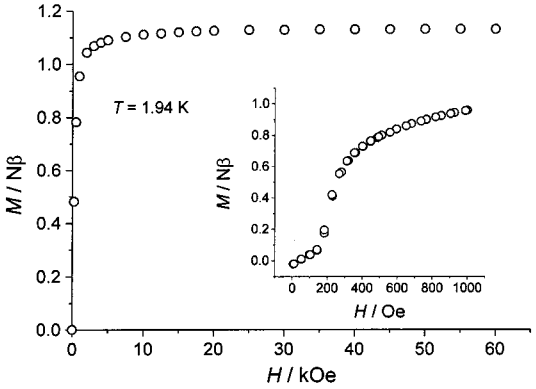

Figure 7. Field dependence of magnetization at 1.9 K for **2**.

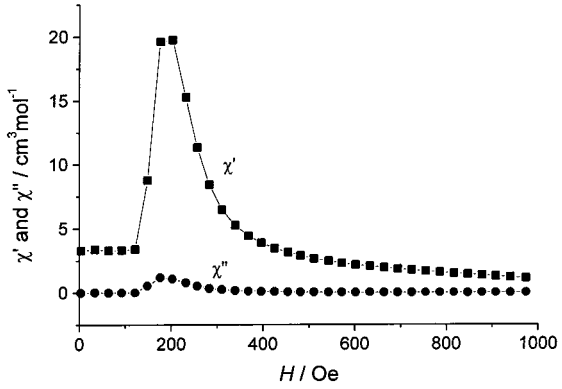

Figure 8. Field dependence of *ac* magnetization at 1.9 K for **2**.

metamagnetic behavior (Figure 7). The saturation magnetization at 60 kOe is 1.13 Nβ per Cu_3 unit, which agrees well with that for **1**. No hysteresis loop was observed at low temperature. The critical field is ~185 Oe, as indicated by the field dependent *ac* susceptibility measurement (Figure 8).

As described, the structures **1** and **2** contain $\{Cu_3(hedp)_2\}_n^{2n-}$ anionic layers separated by $[NH_3(CH_2)_nNH_3]^{2+}$ cations and lattice water. The interlayer distance is 7.48 Å for **1** and 8.20 Å for **2**, respectively. Within the anionic layer, the Cu(II) ions are bridged by O−P−O groups. Although the intralayer interaction through the Cu−O−P−O−Cu exchange pathways is principally antiferromagnetic, the odd number of the Cu(II) ions in the trimer unit leads to a nonzero net magnetic moment. This corresponds to an intralayer ferrimagnetism as observed in the two compounds. Low dimensional ferrimagnetism has also been found in a few other homometallic systems containing discrete

(14) Zheng, L.-M.; Duan, C.-Y.; Ye, X.-R.; Zhang, L.-Y.; Wang, C.; Xin, X.-Q. *J. Chem. Soc., Dalton Trans.* **1998**, 905.

species with an odd number of interacting metal ions.[15] At very low temperature, the antiferromagnetic interaction between the layers dominates, thus leading to an antiferromagnetic ground state at low external fields. This interlayer antiferromagnetic interaction is so weak, however, that a metamagnetic behavior is observed for both **1** and **2**. When the external field approaches to a critical value (∼48 Oe for **1** and 185 Oe for **2**), the compounds switch from an AF ground state to a ferrimagnetic state. The saturation magnetization above 50 kOe (1.18 and 1.13 Nβ per Cu_3 unit for **1** and **2**, respectively) is consistent with the assumption that the exchange within the $\{Cu_3(hedp)_2\}_n^{2n-}$ layer is antiferromagnetic.

In summary, the magnetic properties of two layered copper diphosphonates $[NH_3(CH_2)_4NH_3]Cu_3(hedp)_2 \cdot 2H_2O$ (**1**) and $[NH_3(CH_2)_3NH_3]Cu_3(hedp)_2 \cdot 3.5H_2O$ (**2**) have been reported in this work. Both show a dominant ferrimagnetic behavior within the layer. The weak interlayer antiferromagnetic interaction gives rise to a metamagnetic behavior below 4.7 K for **1** and 6 K for **2**. When a critical field (∼48 Oe for **1** and 185 Oe for **2**) is reached, the compounds switch from an AF ground state to a ferrimagnetic state. To the best of our knowledge, copper phosphonates with metamagnetism have not been previously reported, with the exception of $Cu_4(hedp)_2(pz)(H_2O)_2$, which has a three-dimensional structure.

Acknowledgment. Support from the National Natural Science Foundation of China is gratefully acknowledged. The authors are indebted to Dr. James D. Korp for crystallographic assistance. This work made use of MRSEC/TCSUH Shared Experimental Facilities supported by the National Science Foundation under Award No. DMR-9632667 and the Texas Center for Superconductivity at the University of Houston, USA.

CM020204+

(15) Drillon, M.; Coronado, E.; Belaiche, M.; Carlin, R. L. *J. Appl. Phys.* **1988**, *63*, 3551.